

## Self-Complementary CavitanDs

Adam R. Renslo, Dmitry M. Rudkevich, and Julius Rebek, Jr.\*

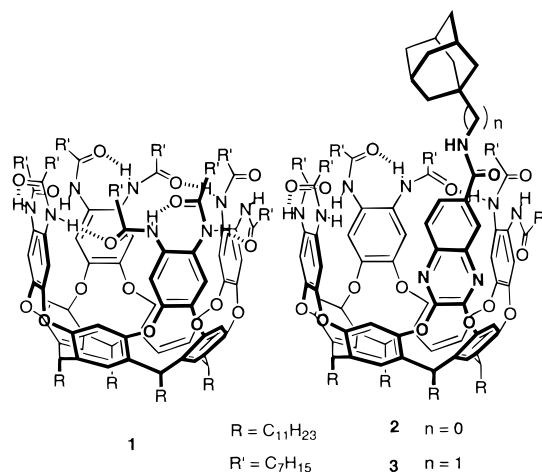
The Skaggs Institute for Chemical Biology and  
The Department of Chemistry  
The Scripps Research Institute  
10550 North Torrey Pines Rd.  
La Jolla, California 92037

Received May 10, 1999

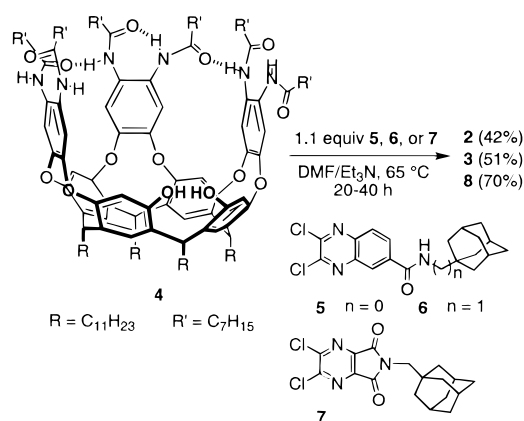
Self-complementarity is ubiquitous in biological macromolecules. The association of two or more copies of, say, a protein gives rise to such structures as allosteric enzymes, viral capsids, and membrane channels.<sup>1,2</sup> Synthetic, self-complementary molecules also show functions unique to their assembled states: recognition, encapsulation, and catalysis are a few recent examples from this laboratory.<sup>3</sup> The driving force in many examples of assembly in organic media not only involves hydrogen bonds, ion–dipole,<sup>4</sup> and other polar interactions but also avoiding voids through the proper filling of cavities. Here we describe a class of molecules that assemble in solution primarily by virtue of self-complementary shapes. These notional “balls in sockets” allow the optimal expression of subtler forces such as van der Waals contacts and C–H/ $\pi$  interactions. Their characteristics as dimeric species offer the first steps along the road to more complex assemblies based on the weakest of intermolecular interactions.<sup>5</sup>

The new molecules are related to the “self-folding” cavitanD hosts (e.g., **1**, Chart 1) described recently.<sup>6</sup> The upper-rim hydrogen-bonding seam in **1** holds the molecule in the vase-like C<sub>4v</sub> conformation and imparts on the resulting caviplexes unusual kinetic stability; guest exchange is slow on the NMR time scale. This kinetic stability is unique among open-cavity receptors and greatly facilitates the study of guest binding. Generally, weak binding affinities ( $\leq 3$  kcal/mol) are observed, even for the best guests, adamantane derivatives. The new cavitanDs **2** and **3** bear covalent links to their guests (Chart 1). As a result, these self-complementary molecules form dimers of considerable kinetic and thermodynamic stability in which the adamantane of one monomer is bound within the cavity of the other.

## Chart 1



## Scheme 1



The ultimately successful strategy for the synthesis of **2**, **3**, and **8** involved hexaamide **4**,<sup>7</sup> as an intermediate. This cavitanD was prepared from Högborg’s resorcinarene<sup>8</sup> in four steps. First, reaction of 1,2-difluoro-4,5-dinitrobenzene (3 equiv) with the resorcinarene octol in DMF/Et<sub>3</sub>N provided the tri-arylated hexanitro cavitanD in 56% yield. A three-step sequence involving reduction (H<sub>2</sub>, Ra–Ni), peracylation (*n*-C<sub>7</sub>H<sub>15</sub>COCl, K<sub>2</sub>CO<sub>3</sub>), and ester cleavage (H<sub>2</sub>NNH<sub>2</sub>, toluene–EtOH) provided cavitanD **4** in 30% overall yield. The <sup>1</sup>H NMR spectrum of **4** is indicative of the folded-vase conformation, even though the hydrogen-bonding seam in **4** is incomplete; one of the four aromatic “walls” of **1** is missing. This breach was then filled by coupling hexaamide **4** to heteroaromatic dichlorides **5**–**7**, to which the adamantanes are attached (Scheme 1).

Figure 1 presents the <sup>1</sup>H NMR spectra of cavitanDs **2**, **3**, and a mixture of **2** and **3** in *p*-xylene-*d*<sub>10</sub> (295 K). Several downfield amide N–H resonances confirm the presence of a hydrogen-bonded seam along the upper rim of the cavitanD. The lower-rim cavitanD methine triplets at 6.3 ppm are diagnostic for the folded-vase conformation. Most telling, however, is the presence of signals in the far upfield region between 0 and –1.5 ppm.<sup>9</sup> These chemical shifts are indicative of adamantane inclusion within the

(1) Nucleic acids: (a) Saenger, W. *Principles of Nucleic Acid Structure*; Springer-Verlag: New York, 1983. Viruses: (b) Klug, A. *Angew. Chem., Int. Ed. Engl.* **1983**, *22*, 565–582. (c) Douglas, T.; Young, M. *Nature* **1998**, *393*, 152–155. Proteins/enzymes: (d) Wlodawer, A.; Miller, M.; Jaskolski, M.; Sathyanarayana, B. K.; Baldwin, E.; Weber, I. T.; Selk, L. M.; Clawson, L.; Schneider, J.; Kent, S. B. H. *Science* **1989**, *245*, 616–621. (e) Dickerson, R. E.; Geis, I. *Hemoglobin: Structure, Function, Evolution, and Pathology*; Benjamin Cumming Publishing: Reading, MA, 1983. (f) Hartgerink, J. D.; Granja, J. R.; Milligan, R. A.; Ghadiri, M. R. *J. Am. Chem. Soc.* **1996**, *118*, 43–50 and references therein. Antibodies: (g) Davies, D. R.; Chacko, S. *Acc. Chem. Res.* **1993**, *26*, 421–427.

(2) Timely reviews on biological and synthetic assemblies: (a) Lawrence, D. S.; Jiang, T.; Levett, M. *Chem. Rev.* **1995**, *95*, 2229–2260. (b) Philp, D.; Stoddart, J. F. *Angew. Chem., Int. Ed. Engl.* **1996**, *35*, 1154–1196. (c) Linton, B.; Hamilton, A. D. *Chem. Rev.* **1997**, *97*, 1669–1680.

(3) (a) Conn, M. M.; Rebek, J., Jr. *Chem. Rev.* **1997**, *97*, 1647. (b) Wintner, E. A.; Rebek, J., Jr. *Acta Chem. Scand.* **1996**, *50*, 469. (c) Rebek, J., Jr. *Acc. Chem. Res.* **1999**, *32*, 278–286.

(4) (a) Yamaguchi, N.; Nagvekar, D., S.; Gibson, H. W. *Angew. Chem., Int. Ed.* **1998**, *37*, 2361. (b) Yamaguchi, N.; Gibson, H. W. *Angew. Chem., Int. Ed.* **1999**, *38*, 143.

(5) In aqueous media, self-aggregation and self-inclusion phenomena have been observed for cyclodextrin derivatives. However, the main driving force in these examples is presumably the hydrophobic effect. For recent examples, see: (a) Gao, X.-M.; Tong, L.-H.; Zhang, Y.-L.; Hao, A.-Y.; Inoue, Y. *Tetrahedron Lett.* **1999**, *40*, 969–972. (b) McAlpine, S. R.; Garcia-Garibay, M. A. *J. Am. Chem. Soc.* **1998**, *120*, 4269–4275 and references therein. (c) Yoshida, N.; Harata, K.; Inoue, T.; Ito; Ichikawa, K. *Supramol. Chem.* **1998**, *10*, 63–67. (d) Kuwabara, T.; Takamura, M.; Matsushita, A.; Ikeda, H.; Nakamura, A.; Ueno, A.; Toda, F. *J. Org. Chem.* **1998**, *63*, 8729–8735.

(6) Rudkevich, D. M.; Hilmersson, G.; Rebek, J., Jr. *J. Am. Chem. Soc.* **1998**, *120*, 12216–12225.

(7) For a synthetic scheme and selected NMR spectra, see Supporting Information. Full experimental details will be published elsewhere.

(8) (a) Högborg, A. G. S. *J. Am. Chem. Soc.* **1980**, *102*, 6046. (b) Högborg, A. G. S. *J. Org. Chem.* **1980**, *45*, 4498.

(9) The complex spectrum observed for **3**•**3** is probably due to the presence of conformational isomers in slow-exchange. Above 320 K, the adamantane signals coalesce to a single set. Chemical exchange of the adamantane nuclei was also supported by the 2D ROESY NMR spectrum of **3**•**3** at 295 K.

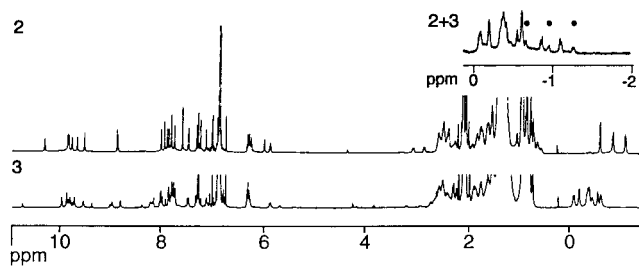


**Figure 1.**  $^1\text{H}$  NMR spectra (600 MHz, 295 K, *p*-xylene- $d_{10}$ , ca. 1 mM) of cavitands **2**, **3**, and a mixture of **2** and **3** (expansion). Adamantane signals arising from **2** in heterodimer **2·3** are marked with solid circles. The corresponding signals arising from **3** in heterodimer **2·3** are not resolved from the signals for homodimer **3·3**.

highly shielded environment of the binding socket.<sup>6</sup> A 2D ROESY NMR spectrum of **2** revealed through-space contacts between the adamantane ball and the aromatic walls of the socket's cavity. Integration of the methine and upfield adamantane resonances indicated that essentially all of the adamantane signals of **2** and **3** lie in this far upfield position. In contrast, no upfield adamantane signals were detected for the imide-linked cavitand **8**. Most probably, a tether of appropriate length between the cavity and the adamantane is crucial and, in the case of **8**, it is simply too short to permit assembly.

The assembly process in **2** and **3** is solvent-dependent. Thus,  $^1\text{H}$  NMR spectra of **2** or **3** in  $\text{CDCl}_3$ , a solvent that competes well for the cavity, revealed that only ca. 20% of the adamantane balls were found within the binding sockets (at 300 K). In DMF- $d_7$ , no adamantane guest was observed in the upfield region of the spectrum. Solvent competition for hydrogen bonds results in rapid fluctuations in the shape (vase to kite)<sup>10</sup> and occupancy of the cavitand.

The further structural details of the assemblies can be inferred from NMR data and computer modeling.<sup>11</sup> The most likely assembly from an entropic standpoint is a dimer. Adamantane self-inclusion, higher aggregates, and even polymeric assemblies are conceivable, however, and must be considered. The possibility of a polymeric assembly seems remote, given the sharp signals observed in NMR spectra of **2** and **3**. Data from the 2D ROESY experiment places the adamantane ball deep in the binding socket, a location that is not obtainable via self-inclusion.<sup>12</sup> The observation of heteroassembly formation (Figure 1) is also incongruous with adamantane self-inclusion. When cavitands **2** and **3** were mixed in *p*-xylene- $d_{10}$  and a  $^1\text{H}$  NMR spectrum was recorded, a new set of adamantane signals (solid circles, Figure 1) was observed in addition to the original signals for **2** and **3**. These new signals are attributed to the formation of a heteroassembly between **2** and **3**. The presence of only one new set of guest signals is most consistent with a dimer: higher-order assemblies, formed with different monomer compositions, should feature more than one set of new guest signals. Computer modeling<sup>13</sup> of a trimer (**3·3·3**) revealed the presence of considerable conformational constraints upon the upper-rim  $\text{C}_7\text{H}_{15}$  chains ( $R'$ ) in the assembly. In contrast, these groups are relatively unencumbered in models of a dimer (Figure 2). We therefore conclude that self-complementary cavitands **2** and **3** form stable dimers in solution. At the millimolar concentrations employed in these experiments, the observation of quantitative guest inclusion (within NMR detection limits) suggests a dimerization constant ( $K_D$ ) of  $\geq 10^5 \text{ M}^{-1}$  in *p*-xylene- $d_{10}$ . In contrast, cavitand **1** binds adamantane

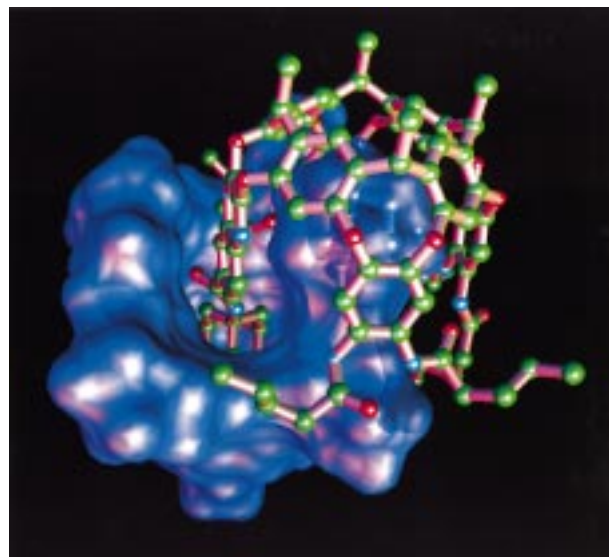


**Figure 2.** Graphic representation of dimer **2·2** based on the minimized structure obtained from MacroModel 5.5 (Amber\* force field). The solvent-accessible surface of one monomer is rendered in blue, while the other is depicted as a ball-and-stick model. The  $n\text{-C}_{11}\text{H}_{23}$  chains ( $R$ ) are substituted by  $\text{CH}_3$  and the  $n\text{-C}_7\text{H}_{15}$  chains ( $R'$ ) by  $n\text{-C}_4\text{H}_9$ .

guests with association constants ( $K_{\text{ass}}$ ) that are typically  $\leq 10^2 \text{ M}^{-1}$  in this solvent.<sup>6</sup>

In *p*-xylene, the spherical adamantane guest is a better fit for the socket's cavity than is a solvent molecule. When a dimer forms, both cavities are better filled and (at least) two solvent molecules are released into the bulk solution. However, the thermodynamic parameters of the process could not be determined in *p*-xylene since *only* dimer was observed in the temperature regime between 295 and 340 K. In  $\text{CDCl}_3$ , the assembly is much weaker, and the equilibrium process can be followed directly by variable temperature NMR. From integration of the bound adamantane and the methine signals in **2**, the dimerization constants were calculated; for example a  $K_D$  value of  $250 \text{ M}^{-1}$  at 300 K was obtained ( $\Delta G^{300} = -3.3 \text{ kcal/mol}$ ). Temperature effects on  $K_D$  were measured, and a van't Hoff plot provided the corresponding thermodynamic parameters of  $\Delta H = -10.6 \text{ kcal/mol}$  and  $\Delta S = -24.5 \text{ eu}$ . Accordingly, the dimerization process is enthalpically favorable and entropically unfavorable.

In conclusion, a self-complementary cavity-guest binding motif may result in strong self-association, even when weak attracting forces are employed. The binding affinity observed for dimers **2·2** and **3·3** is markedly higher than is the binding of adamantane guests by **1** ( $\Delta\Delta G^{295} \geq 4 \text{ kcal/mol}$  in *p*-xylene) and even a large excess of external adamantane guest ( $\geq 10$  equiv) does not disrupt the assembly. The increased binding affinity is likely a result of the cooperation of binding sites inherent to self-complementary molecules. The dimers **2·2** and **3·3** are early examples of assemblies that form without intermolecular hydrogen bonding networks between the subunits. We also remind the readers that self-complementarity is the signature of synthetic, self-replicating systems.<sup>3b</sup>

**Acknowledgment.** We thank Dr. Paul L. Wash for the molecular graphic and Dr. Laura Pasternack for assistance with 2D NMR experiments. We are grateful to the Skaggs Foundation and the National Institutes of Health for support of this work.

**Supporting Information Available:** Synthetic scheme for hexamide **4**, NMR spectra of **4**, the hexanitro intermediate, and cavitands **2** and **3** (including 2D ROESY spectrum of **2**), and van't Hoff plot for assembly of **2·2** in  $\text{CDCl}_3$  (PDF). This material is available free of charge via the Internet at <http://pubs.acs.org>.

(10) Moran, J. R.; Ericson, J. L.; Dalcanale, E.; Bryant, J. A.; Knobler, C. B.; Cram, D. J. *J. Am. Chem. Soc.* **1991**, *113*, 5707.

(11) To date, all attempts to characterize the assembly using ESI, FAB, and MALDI-TOF mass spectrometry have been unsuccessful.

(12) The tether between adamantane and quinoxaline is not long enough for the adamantane moiety to occupy the binding cavity intramolecularly, even if the amide bond in the tether is held in the (disfavored) *cis* conformation.

(13) Amber\* force field; MacroModel 5.5.